Improved Multi-goal Particle Swarm Optimization Algorithm and Multi-output BP Network for Optimal Operation of Power System

Jie Qian and Gonggui Chen*

Abstract—**To achieve the optimal operation of power system, an improved multi-goal particle swarm optimization (IMPSO) algorithm is proposed in this paper. Based on the multi-goal optimal power flow (MOOPF) calculation, IMPSO algorithm can determine high-quality scheduling schemes which effectively reduce fuel cost, power loss and exhaust emission. Compared with the basic multi-goal PSO (BMPSO) algorithm, IMPSO algorithm realizes better solution diversity and searching ability by integrating an innovative dominant strategy and the mutation-crossover operation of inferior solutions. Four experiments prove that the proposed IMPSO algorithm achieves more superior Pareto optimal set (POS) and best compromise scheme (BCS) than BMPSO algorithm. Furthermore, the multi-output BP power flow prediction model is put forward in this paper to seek the winning elite schemes (WES) around the BCS of IMPSO algorithm. The presented BP prediction model can find multiple WES schemes of bi-objective and tri-objective MOOPF problems, which realize zero constraint violation and smaller goals. In general, the superior WES schemes determined by proposed IMPSO and BP power flow prediction model are of great help to realize the optimal operation of power system with improved economy and safety.**

Index Terms—**Particle swarm optimization, Optimal power flow, BP prediction model, Optimal operation**

I. Introduction

As an important energy, electric energy plays a key role in maintaining daily life. The optimal power flow (OPF) research can reduce the fuel cost, exhaust emission and power loss [1-3], which contributes to realize the better operation of power system. Furthermore, compared with single-objective OPF, the multi-goal OPF (MOOPF) research which can optimize more than two goals at the same time is more concerned by scholars.

However, the high dimensional and non-differentiable characteristics make traditional methods not suitable for MOOPF problems. The advanced computer technologies represented by intelligent algorithms and neural networks provide great inspiration for efficiently solving MOOPF problems. For example, the QOMJaya method with quasi -oppositional based learning [4], the NSGA-FA algorithm with special sorting rule and location-updating mechanism [5], the FAHSPSO-DE algorithm with fuzzy adaptive hybrid configuration [6] have smoothly solved MOOPF problems.

A review of literatures shows that these algorithms suitable for MOOPF problems require satisfactory population diversity and excellent searching ability. Particle swarm optimization (PSO) algorithm as a representative swarm intelligence algorithm has wide application and good robustness. In recent years, PSO algorithm has solved many complex optimizations in power system such as the forecast of satellite power system parameter interval [7] and the power system network reconfiguration [8]. Therefore, PSO algorithm has the potential to deal with complex MOOPF problems.

A. Contributions

It is worth noting that, there are two key points in solving MOOPF problems with PSO algorithm. Firstly, an effective dominant strategy is indispensable to evaluate different scheduling schemes with m ($m \geq 2$) goals. In this paper, a constraint-goal dominant strategy considering constraint violation and candidate goal is put forward. Integrating the presented constraint-goal dominant strategy into the single objective PSO algorithm model can generate the basic multi-goal PSO (BMPSO) algorithm, which is used as the comparison algorithm in this paper. Then, in order to obtain high-quality Pareto optimal set (POS) and best compromise scheme (BCS) of MOOPF, two other improvements are combined with BMPSO to form the proposed improved multi-goal PSO (IMPSO) algorithm.

Besides the constraint-goal dominant strategy, the additional local exploration operation and mutation crossover operation of inferior solutions greatly improve the population diversity and optimization performance of IMPSO algorithm. Compared with BMPSO algorithm, the suggested IMPSO algorithm has better running stability and is capable to determine feasible BCS schemes with clear competitive advantage.

Furthermore, a multi-output BP power flow network which can predict the fuel cost, power loss and emission of MOOPF problems is constructed in this paper. The proposed BP prediction model can quickly find the winning elite schemes (WES) of MOOPF problems in a small range near the obtained BCS. The WES schemes should satisfy all system constraints and have m smaller goals than current BCS, which

Manuscript received December 21, 2021; revised May 16, 2022. This work was supported by the Doctoral Talent Training Project of Chongqing University of Posts and Telecommunications under Grant BYJS202113.

Jie Qian is a PhD candidate of School of Computer Science and Technology, Chongqing University of Posts and Telecommunications, Chongqing 400065, China (e-mail: qianjie@126.com).

Gonggui Chen is a professor of Key Laboratory of Industrial Internet of Things and Networked Control, Ministry of Education, Chongqing University of Posts and Telecommunications, Chongqing 400065, China (corresponding author, e-mail: chenggpower@163.com).

are beneficial to achieve the optimal operation of power system.

B. Structure

The structure of this paper is set as follows. Three components of MOOPF including goals, constraints and constraint handling strategy are given in Section II. Then, Section III gives the improvements and application of proposed IMPSO algorithm. Four experiments prove the advantages of IMPSO algorithm in obtaining better BCS and running stability when solving MOOPF problems. Besides, the application of proposed BP power flow prediction model on bi-objective and tri-objective MOOPF problems is given in Section IV. Finally, Section V gives the conclusion of this paper.

II. Mathematical Model

Four goals of MOOPF problems are studied in this paper. Each available power flow dispatching scheme should satisfy all system constraints. Therefore, the appropriate constraint processing method is also an important part of MOOPF mathematical model.

A. Goals

The novel IMPSO algorithm is put forward to determine the qualified dispatching schemes which reduce power loss (G_{pl}), basic fuel cost (G_{fc}), fuel cost with valve point effect (G_{fv}) and emission (G_e). The mentioned goals are shown as (1) ~ (4) [9, 10].

$$G_{pl} = \sum_{k=1}^{N_L} con_{(k)}[V_i^2 + V_j^2 - 2V_iV_j\cos(\delta_i - \delta_j)]\ MW \quad (1)$$

$$G_{fc} = \sum_{i=1}^{N_G}(a_i + b_iP_{Gi} + c_iP_{Gi}^2)\ \$/h \quad (2)$$

$$G_{fv} = \sum_{i=1}^{N_G}(a_i + b_iP_{Gi} + c_iP_{Gi}^2 + \left|d_i \times \sin(e_i \times (P_{Gi}^{\min} - P_{Gi}))\right|)\ \$/h \quad (3)$$

$$G_e = \sum_{i=1}^{N_G}[\alpha_iP_{Gi}^2 + \beta_iP_{Gi} + \gamma_i + \eta_i\exp(\lambda_iP_{Gi})]\ ton/h \quad (4)$$

where $con_{(k)}$ is the conductance of kth branch. N_L and N_G are the numbers of transmission lines and generators. V and δ are the amplitude and phase angle of voltage, respectively. a, b, c, d and e are five cost coefficients while α, β, γ, η and λ are emission coefficients. In addition, P_{Gi} is the active power of ith node.

B. Constraints

The constraints of MOOPF problems include two equality constraints and two kinds of inequality constraints. Two equality constraints show the active power balance and reactive one. The inequality constraints of control variables act on generator active power output at PV node (P_G), generator node voltage (V_G), transformer (T) and reactive power injection (Q_C). Meanwhile, the inequality constraints of state variables act on generator active power at slack node (P_{G1}), load node voltage (V_L), generator reactive power (Q_G) and apparent power of transmission line (S).

The above system constraints of MOOPF problems can be found in [11, 12]. Two equality constraints are used as the termination condition of Newton-Raphson calculation. Thus, this paper focuses on the treatment strategy of inequality constraints.

C. Constraints processing

As independent variables of MOOPF problems, the control variables which do not satisfy inequality constraints will be adjusted according to formula (5).

$$Vc_i = \begin{cases} Vc_i^{min} & ,Vc_i < Vc_i^{min} \\ Vc_i^{max} & ,Vc_i > Vc_i^{max} \end{cases} \quad (5)$$

where Vc_i^{min}=[P_G^{min}, V_G^{min}, T^{min}, Q_C^{min}] and Vc_i^{max}=[P_G^{max}, V_{Gi}^{max}, T^{max}, Q_C^{max}] define the valid ranges of ith control variables set (Vc).

Additionally, the constraint violation ($Viol$) of unqualified state variables defined as (6) is used as one criterion of adoption priority of different scheduling schemes.

$$Viol(S_i) = |Viol_P(S_i)| + |Viol_V(S_i)| + |Viol_Q(S_i)| + |Viol_S(S_i)| \quad (6)$$

where $Viol_P(S_i)$, $Viol_V(S_i)$, $Viol_Q(S_i)$ and $Viol_S(S_i)$ are the violations of the ith scheme (S_i) which violates the inequality constraints of P_{G1}, V_L, Q_G and S, respectively.

III. IMPSO Algorithm and Application

To smoothly solve the complex MOOPF problems with m conflicting goals, the original single-objective PSO algorithm needs to be combined with effective non-inferior dominance rule of different dispatching schemes. In this paper, the BMPSO algorithm which is able to find the feasible POS of MOOPF is generated by integrating constraint-goal dominant strategy.

A. BMPSO algorithm

The velocity with inertia weight and position update formulas of BMPSO algorithm are shown as (7) and (8). Meanwhile, the inertia weight is updated based on (9).

$$v_i^{k+1} = \omega^k v_i^k + c_1r_1(x_p - x_i^k) + c_2r_2(x_g - x_i^k) \quad (7)$$

$$x_i^{k+1} = x_i^k + v_i^{k+1} \quad (8)$$

$$\omega^k = \omega_s - (\omega_s - \omega_e)k \Big/ k^{\max} \quad (9)$$

where c_1, c_2 are two learning factors and r_1, r_2 are random numbers between (0, 1). x_p and x_g indicate the current local optimum and global one. ω_s and ω_e are the maximum and minimum of inertia weight. And k^{max} is the maximum iteration.

For specific MOOPF problems, the constraint-goal dominant strategy is also integrated into BMPSO algorithm. The proposed constraint-goal dominant strategy aims to select the final POS set of MOOPF problems based on goal values and constraint violation.

Firstly, the $Rank$ index of each candidate power flow scheme is determined based on the non-inferior sorting rule proposed by Deb [13, 14]. In detail, it can be judged that the S_i scheme dominates the S_j one when condition (10) or (11) is satisfied.

Among Na candidate schemes, these elite schemes that are not dominated by any other scheme are marked as $Rank$=1. Regardless of the schemes with definite $Rank$ index, these suboptimal schemes with $Rank$=2 are also determined according to (10) and (11). Repeat the above process until all Na candidate schemes have their corresponding $Rank$ index. In this paper, $R_{(i)}$ represents the number of schemes with $Rank \le i$, and Np is the scale of POS set.

$$Viol(S_i) < Viol(S_j) \tag{10}$$

$$\begin{cases} Viol(S_i) = Viol(S_j) \\ f_p(S_i) \le f_p(S_j), \forall p \in \{1,2,...,m\} \\ f_q(S_i) < f_q(S_j), \exists q \in \{1,2,...,m\} \end{cases} \tag{11}$$

When $R_{(i-1)} < Np$ and $R_{(i)} > Np$, the ($R_{(i)}$- Np) schemes with better performance are determined from the candidate schemes with $Rank=i$ and included in the final POS set. After clarifying the *Rank* index according to constraint-goal dominant strategy, the POS of MOOPF problems can be determined as follows.

(*i*) According to the satisfaction function shown in formulas (12) and (13), a relatively optimal scheduling scheme BCS_R is determined from the $R_{(1)}$ dominant schemes with $Rank=1$. The detail of satisfaction function can be found in [12, 15].

$$Ffuz_i^j = \begin{cases} 1 & f_i \le f_i^{\min} \\ \dfrac{f_i^{\max} - f_i}{f_i^{\max} - f_i^{\min}} & f_i^{\min} < f_i < f_i^{\max} \\ 0 & f_i \ge f_i^{\max} \end{cases} \tag{12}$$

$$i = 1,2,\ldots,m \quad j = 1,2,\ldots Np$$

$$Fsat(j) = \frac{\sum_{i=1}^{m} Ffuz_i^j}{\sum_{j=1}^{Np}\sum_{i=1}^{m} Ffuz_i^j} \tag{13}$$

where $f_i^{\max}$ and $f_i^{\min}$ are the maximum and minimum of *i*th goal.

(*ii*) Calculate the Euclidean distances (D_{Euc}) between the ($R_{(i)}$-$R_{(i-1)}$) schemes with $Rank=i$ and BCS_R scheme, respectively.

(*iii*) The ($R_{(i)}$-Np) schemes with smaller D_{Euc} are selected from ($R_{(i)}$-$R_{(i-1)}$) candidate schemes and included into POS set.

(*iv*) Determine the final POS set which is composed by the above ($R_{(i)}$- Np) schemes with $Rank=i$ and $R_{(i-1)}$ schemes with $Rank \le i$-1.

In general, the above BMPSO algorithm with constraint-goal dominant strategy is capable to handle MOOPF problems.

B. Proposed IMPSO algorithm

Experiments show that BMPSO algorithm can obtain feasible POS. However, the uniformity of Pareto Front (PF) and the quality of BCS schemes still have room for improvement. Therefore, besides the proposed constraint goal dominant strategy, IMPSO algorithm also integrates local exploration operation and mutation crossover operation to further optimize the performance of solving MOOPF problems.

1) Local exploration operation

In order to improve the population diversity, the local exploration operation is supplemented in the suggested IMPSO algorithm. Specifically, the local exploration operation shown as (14) is performed on the current Np solutions for each 50 iteration.

$$x_i^{new} = x_i^{original} + r_3 x_i^{original}, i = 1,2,\cdots,Np \tag{14}$$

where $x_i^{original}$ is the original individual at *k*th (k=50,100,…, k^{max}) iteration and r_3 is a random number between (-1,1).

After the local search operation is completed, Np $x^{original}$ schemes and Np x^{new} ones are integrated and duplicate solutions are deleted to obtain Nv ($Np \le Nv \le 2Np$) candidate schemes. The *Rank* index of Nv schemes and the D_{Euc} distance of corresponding candidate solutions are clarified first. Then, the Np schemes with better quality determined based on constraint-goal dominant strategy are selected for the next iteration.

2) Mutation-crossover operation

The current POS set of MOOPF problems can be obtained by presented IMPSO algorithm after k^{max} iteration. In this paper, the Ni scheduling schemes with largest *Rank* index in POS set is defined as inferior schemes. The mutation crossover operation shown in (15) and (16) is implemented on inferior schemes to improve the quality of POS set. In addition, at least 20%Np schemes perform the mutation crossover operation in this paper. If Ni < 20%Np, the (20%Np -Ni) random schemes with lower adoption priority are also perform this operation to further optimize the variety and performance of scheduling schemes. The mutation crossover operation is inspired by differential evolution algorithm and the details can be referred to [16, 17].

$$x_{mu}(i) = x_{S1} + F_{mu}(x_{S2} - x_{S3}), i = 1,2,\cdots N_i \tag{15}$$

$$x_{cr}(i) = \begin{cases} x_{mu}(i), & if\ \eta \le F_{cr}\ or\ j = q \\ x_i, & otherwise \end{cases} \quad j = 1,2,\cdots,D \tag{16}$$

where x_{S1}, x_{S2} and x_{S3} are three different schemes. F_{mu} and F_{cr} are, respectively, the mutation factor and crossover one. η is a random number between 0 and 1. D is the dimension of independent variables and q is a positive integer between [1, D].

C. Application of IMPSO algorithm

The innovative IMPSO algorithm is put forward by integrating the above three improvements and the main flow of IMPSO algorithm to solve MOOPF problems is shown in Fig. 1.

To verify the applicability and advantages of IMPSO algorithm, four MOOPF simulation experiments shown in TABLE I are carried out in this paper.

1) Case 1

In this paper, Case 1 simultaneously considers the reduction of power loss and basic fuel cost on IEEE 30-bus system. The structure and details of standard IEEE 30-bus system can be found in [12, 18].

The PFs of Case 1 obtained by BMPSO and IMPSO algorithms are shown in Fig. 2. Fig. 2 indicates that the proposed IMPSO algorithm determines the uniformly distributed PF while the PF of BMPSO algorithm is relatively scattered.

TABLE I
CASE SETTINGS

Cases	Goals	*m*	System	Number of independent experiments
Case 1	G_{fc} & G_{pl}	2	IEEE 30	30
Case 2	G_{fv} & G_{pl}	2	IEEE 30	30
Case 3	G_{fc} & G_{pl} & G_e	3	IEEE 30	30
Case 4	G_{fc} & G_{pl}	2	IEEE 57	30

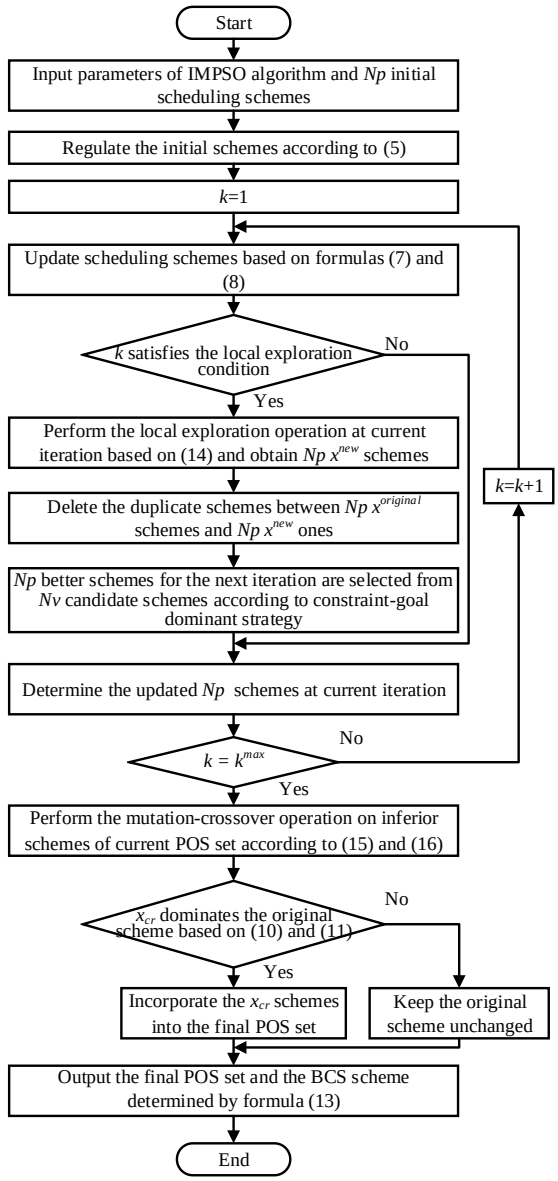

Fig. 1. IMPSO algorithm on MOOPF problems

Furthermore, Fig. 2 also gives the objectively determined BCS scheme and two schemes which respectively obtain the minimum cost and minimum power loss. It clearly states that IMPSO algorithm achieves the minimum power loss with 2.8547 MW and the minimum fuel cost with 799.3476 $/h. For Case 1, the 24-dimensional control variables of specific schemes are given in TABLE II. TABLE II shows that the BCS of IMPSO algorithm including 5.0715 MW of power loss and 831.2837 $/h of fuel cost is obviously better than the one of BMPSO algorithm including 5.1425 MW of power loss and 836.4278 $/h of fuel cost.

The PF-uniformity and BCS-quality show the effectiveness of three improvements and the competitive advantage of proposed IMPSO algorithm in solving dual-objective MOOPF problems.

2) Case 2

In Case 2, the power loss and fuel cost with valve-point are optimized at the same time on IEEE 30-bus system. The valve-point effect increases the difficulty of solving MOOPF problems, which is also the main reason that intelligent algorithms are adopted instead of traditional methods to solve MOOPF problems.

Fig. 3 gives the PFs of Case 2 and states the PF uniformity of IMPSO algorithm is more superior to the one of BMPSO algorithm. Fig. 3 also shows IMPSO algorithm obtains the minimum power loss with 2.8410 MW and the minimum fuel cost considering valve-point with 831.3622 $/h. Besides, the presented IMPSO algorithm finds the BCS scheme composed by 5.6685 MW of power loss and 863.3560 $/h of fuel cost considering valve-point. TABLE III gives the detail control variables of corresponding scheduling schemes for Case 2.

In general, Fig. 3 and TABLE III intuitively prove the superiorities of IMPSO algorithm put forward in this paper for solving complex MOOPF problems compared with the basic BMPSO algorithm.

3) Case 3

In contrast to the dual-objective optimizations, the tri-objective MOOPF problems with greater difficulty can evaluate the performance of novel IMPSO algorithm more comprehensively.

The Case 3 in this paper aims to realize the simultaneous optimization of power loss, emission and fuel cost on IEEE 30-bus system. The PFs of Case 3 obtained by BMPSO and IMPSO algorithms are given in Fig. 4 and Fig. 5, respectively. It indicates that BMPSO algorithm obtains the feasible POS set, but the PF-uniformity is not as good as that of IMPSO algorithm. Additionally, Fig. 5 shows the distribution of three scheduling schemes with minimum single goal obtained by IMPSO algorithm. In detail, IMPSO algorithm achieves the minimum emission with 0.1942 ton/h, the minimum power loss with 2.8544 MW and the minimum fuel cost with 799.1717 $/h.

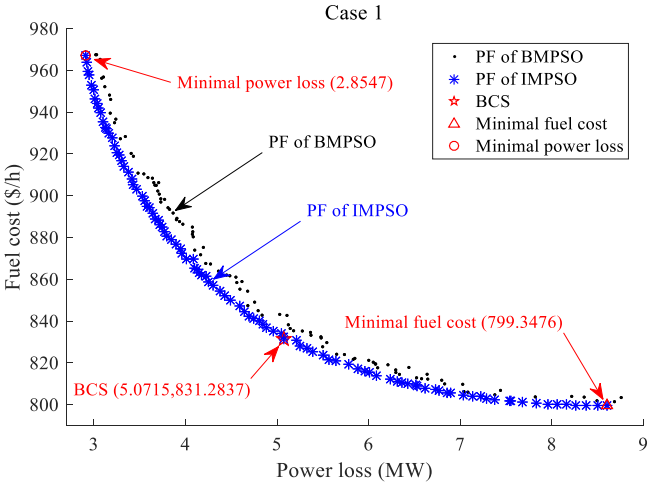

Fig. 2. PFs of Case 1

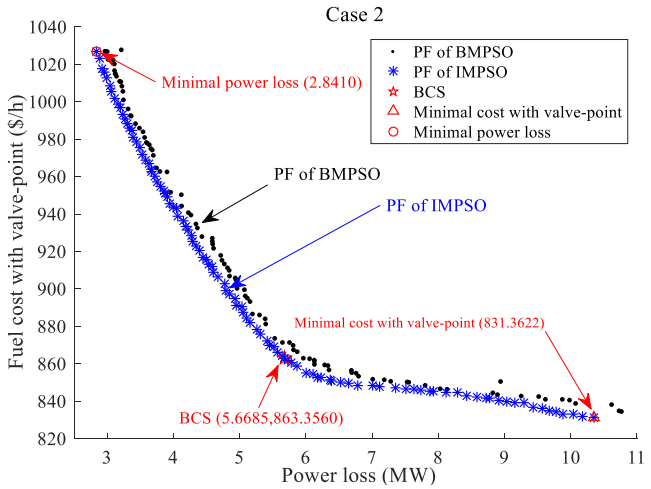

Fig. 3. PFs of Case 2

TABLE II
CONTROL VARIABLES OF SCHEDULING SCHEMES IN CASE 1

Case 1	BCS		Schemes with minimum single goal of IMPSO	
Variables	BMPSO	IMPSO	Minimum fuel cost	Minimum power loss
P_{G2}(MW)	54.4895	52.7942	48.2721	80.0000
P_{G5}(MW)	36.2669	30.8092	21.2022	50.0000
P_{G8}(MW)	33.6890	34.8318	23.2476	35.0000
P_{G11}(MW)	27.3292	27.6957	10.7979	30.0000
P_{G13}(MW)	16.4369	23.0659	12.0313	40.0000
V_{G1}(p.u.)	1.1000	1.1000	1.0998	1.1000
V_{G2}(p.u.)	1.0902	1.0909	1.0876	1.0985
V_{G5}(p.u.)	1.0694	1.0696	1.0638	1.0848
V_{G8}(p.u.)	1.0692	1.0774	1.0671	1.0897
V_{G11}(p.u.)	1.0895	1.0947	1.0961	1.0875
V_{G13}(p.u.)	1.0660	1.0997	1.0714	1.1000
T_{11}(p.u.)	1.0131	1.0464	1.0453	1.0061
T_{12}(p.u.)	0.9622	0.9347	0.9382	0.9574
T_{15}(p.u.)	0.9646	0.9949	1.0112	0.9782
T_{36}(p.u.)	0.9696	0.9828	0.9824	0.9709
Q_{C10}(p.u.)	0.0196	0.0470	0.0013	0.0500
Q_{C12}(p.u.)	0.0276	0.0002	0.0180	0.0000
Q_{C15}(p.u.)	0.0187	0.0273	0.0329	0.0423
Q_{C17}(p.u.)	0.0042	0.0497	0.0300	0.0500
Q_{C20}(p.u.)	0.0363	0.0477	0.0384	0.0453
Q_{C21}(p.u.)	0.0500	0.0495	0.0220	0.0500
Q_{C23}(p.u.)	0.0116	0.0301	0.0292	0.0388
Q_{C24}(p.u.)	0.0398	0.0484	0.0431	0.0483
Q_{C29}(p.u.)	0.0329	0.0263	0.0278	0.0259
G_{pl}(MW)	5.1425	**5.0715**	8.6182	**2.8547**
G_{fc}(\$/h)	836.4278	**831.2837**	**799.3476**	967.0772

TABLE III
CONTROL VARIABLES OF SCHEDULING SCHEMES IN CASE 2

Case 2	BCS		Schemes with minimum single goal of IMPSO	
Variables	BMPSO	IMPSO	Minimum cost with valve-point	Minimum power loss
P_{G2}(MW)	45.9942	45.7978	45.4282	80.0000
P_{G5}(MW)	29.3674	32.0684	18.2797	50.0000
P_{G8}(MW)	34.4707	34.9037	10.0000	35.0000
P_{G11}(MW)	26.6746	23.4431	10.0000	30.0000
P_{G13}(MW)	19.3145	17.1178	12.0000	40.0000
V_{G1}(p.u.)	1.1000	1.1000	1.1000	1.0986
V_{G2}(p.u.)	1.0798	1.0866	1.0833	1.0978
V_{G5}(p.u.)	1.0676	1.0664	1.0501	1.0775
V_{G8}(p.u.)	1.0616	1.0756	1.0564	1.0862
V_{G11}(p.u.)	1.0860	1.1000	1.0580	1.1000
V_{G13}(p.u.)	1.0928	1.1000	1.0695	1.1000
T_{11}(p.u.)	1.0993	1.0646	1.0430	1.0122
T_{12}(p.u.)	0.9125	0.9005	0.9390	0.9524
T_{15}(p.u.)	1.0068	0.9935	1.0369	0.9888
T_{36}(p.u.)	0.9889	0.9749	1.0109	0.9726
Q_{C10}(p.u.)	0.0186	0.0211	0.0000	0.0500
Q_{C12}(p.u.)	0.0192	0.0175	0.0000	0.0500
Q_{C15}(p.u.)	0.0500	0.0321	0.0220	0.0404
Q_{C17}(p.u.)	0.0315	0.0458	0.0437	0.0500
Q_{C20}(p.u.)	0.0267	0.0482	0.0492	0.0478
Q_{C21}(p.u.)	0.0183	0.0500	0.0279	0.0500
Q_{C23}(p.u.)	0.0495	0.0225	0.0205	0.0285
Q_{C24}(p.u.)	0.0144	0.0496	0.0197	0.0500
Q_{C29}(p.u.)	0.0500	0.0301	0.0500	0.0280
G_{pl}(MW)	5.8706	**5.6685**	10.3532	**2.8410**
G_{fv} (\$/h)	866.4884	**863.3560**	**831.3622**	1026.6280

Furthermore, TABLE IV, which gives the control variables of tri-objective scheduling schemes, indicates IMPSO algorithm determines the BCS schemes including 0.2131 ton/h of emission, 4.3958 MW of power loss and 863.2721 $/h of fuel cost. Obviously, the BCS of IMPSO algorithm is more preferable than the one of BMPSO algorithm which includes 0.2131 ton/h of emission, 4.3964 MW of power loss and 869.7383 $/h of fuel cost. And the advantage of the BCS obtained by IMPSO algorithm is mainly embodied in the reduction of fuel cost.

4) Case 4

Further, the effectiveness of IMPSO algorithm for MOOPF problems is also verified on the more complex IEEE 57-bus system with 33 dimensional control variables. The Case 4 considers the simultaneous reduction of power loss and fuel cost on IEEE 57-bus system. The structure and details of standard 57-bus system can be found in [19, 20].

The PFs of Case 4 obtained by BMPSO and IMPSO are shown in Fig. 6. Fig. 6 shows that IMPSO algorithm obtains the uniformly distributed PF while BMPSO algorithm finds a scattered one. Besides, Fig. 6 indicates on IEEE 57-bus system, IMPSO algorithm achieves the minimum power loss with 9.6184 MW and the minimum fuel cost with 41672.8007 $/h. The control variables of BCS schemes and two schemes with minimum single goal are given in TABLE V. TABLE V states that IMPSO algorithm achieves the BCS scheme including 10.9830 MW of power loss and 41988.2811 $/h of fuel cost, which dominates BMPSO algorithm.

Case 4 states that the advantages of IMPSO in obtaining the uniformly distributed PF and high quality BCS are more fully reflected in high-dimensional 57-bus system.

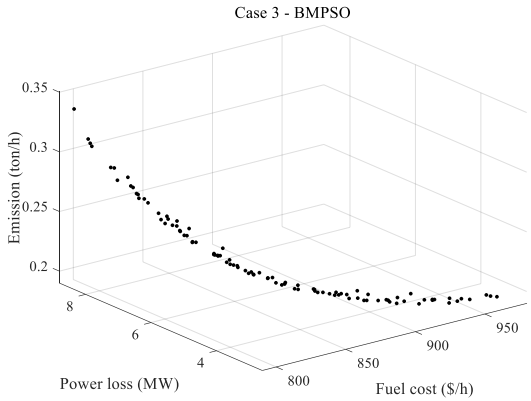

Fig. 4. PF of BMPSO algorithm for Case 3

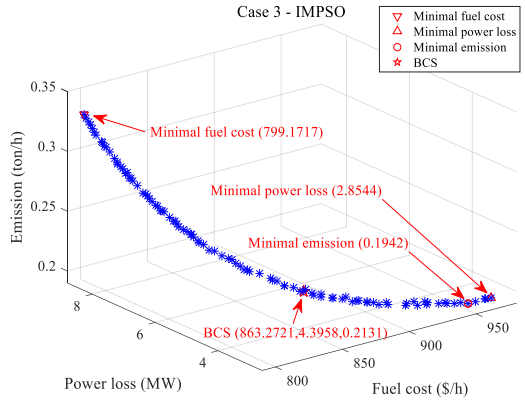

Fig. 5. PF of IMPSO algorithm for Case 3

TABLE IV
CONTROL VARIABLES OF SCHEDULING SCHEMES IN CASE 3

Case 3	BCS		Schemes with minimum single goal of IMPSO		
Variables	BMPSO	IMPSO	Minimum fuel cost	Minimum power loss	Minimum emission
P_{G2}(MW)	57.9676	62.1318	48.1791	80.0000	72.4413
P_{G5}(MW)	39.4766	35.9530	21.1218	50.0000	50.0000
P_{G8}(MW)	31.7923	34.4143	22.0236	35.0000	35.0000
P_{G11}(MW)	29.7538	29.4704	11.3591	30.0000	30.0000
P_{G13}(MW)	31.5219	29.8920	12.0450	40.0000	40.0000
V_{G1}(p.u.)	1.0977	1.1000	1.1000	1.1000	1.1000
V_{G2}(p.u.)	1.0893	1.0902	1.0881	1.0974	1.0980
V_{G5}(p.u.)	1.0786	1.0852	1.0594	1.0807	1.0770
V_{G8}(p.u.)	1.0765	1.0861	1.0698	1.0896	1.0877
V_{G11}(p.u.)	1.0594	1.0786	1.0978	1.0914	1.1000
V_{G13}(p.u.)	1.0108	1.1000	1.1000	1.1000	1.1000
T_{11}(p.u.)	1.0977	1.0083	0.9369	1.0831	1.0912
T_{12}(p.u.)	1.0183	0.9048	1.0513	0.9000	0.9000
T_{15}(p.u.)	1.1000	1.0673	1.0216	0.9775	0.9899
T_{36}(p.u.)	1.0563	0.9868	0.9831	0.9783	0.9755
Q_{C10}(p.u.)	0.0500	0.0316	0.0031	0.0500	0.0500
Q_{C12}(p.u.)	0.0149	0.0017	0.0469	0.0000	0.0000
Q_{C15}(p.u.)	0.0446	0.0331	0.0306	0.0456	0.0500
Q_{C17}(p.u.)	0.0500	0.0490	0.0422	0.0470	0.0435
Q_{C20}(p.u.)	0.0204	0.0487	0.0448	0.0401	0.0428
Q_{C21}(p.u.)	0.0488	0.0489	0.0377	0.0500	0.0500
Q_{C23}(p.u.)	0.0430	0.0489	0.0413	0.0500	0.0500
Q_{C24}(p.u.)	0.0056	0.0130	0.0305	0.0413	0.0298
Q_{C29}(p.u.)	0.0048	0.0092	0.0376	0.0226	0.0209
G_e(ton/h)	0.2131	**0.2131**	0.3296	0.1949	**0.1942**
G_{pl} (MW)	4.3964	**4.3958**	8.6474	**2.8544**	2.9348
G_{fv} ($/h)	869.7383	**863.2721**	**799.1717**	967.0766	952.1179

TABLE V
CONTROL VARIABLES OF SCHEDULING SCHEMES IN CASE 4

Case 4 Variables	BCS		Schemes with minimum single goal of IMPSO	
	BMPSO	IMPSO	Minimum fuel cost	Minimum power loss
P_{G2}(MW)	86.9564	77.7233	94.7361	0.0000
P_{G3}(MW)	68.2585	57.3050	44.7901	140.0000
P_{G6}(MW)	79.6996	91.3638	74.0569	99.6210
P_{G8}(MW)	365.1545	374.0779	458.6700	305.2403
P_{G9}(MW)	99.8420	99.5810	83.3328	99.9532
P_{G12}(MW)	410.0000	408.8989	366.3933	409.8839
V_{G1}(p.u.)	1.1000	1.1000	1.1000	1.1000
V_{G2}(p.u.)	1.1000	1.0976	1.0977	1.0950
V_{G3}(p.u.)	1.1000	1.0920	1.0886	1.1000
V_{G6}(p.u.)	1.1000	1.1000	1.1000	1.1000
V_{G8}(p.u.)	1.1000	1.1000	1.1000	1.1000
V_{G9}(p.u.)	1.1000	1.0933	1.0874	1.0948
V_{G12}(p.u.)	1.1000	1.0933	1.0866	1.0949
T_{19}(p.u.)	0.9712	0.9538	0.9555	0.9710
T_{20}(p.u.)	1.0280	1.0625	1.0957	1.0353
T_{31}(p.u.)	0.9995	0.9640	0.9502	0.9775
T_{35}(p.u.)	0.9969	0.9991	1.0946	0.9346
T_{36}(p.u.)	1.1000	0.9582	0.9386	0.9933
T_{37}(p.u.)	1.0958	0.9631	0.9864	0.9510
T_{41}(p.u.)	1.0871	1.0071	1.0265	0.9980
T_{46}(p.u.)	0.9265	0.9641	0.9646	0.9677
T_{54}(p.u.)	0.9477	0.9843	1.0013	0.9717
T_{58}(p.u.)	1.0144	1.0037	1.0061	0.9996
T_{59}(p.u.)	0.9917	1.0259	1.0467	1.0091
T_{65}(p.u.)	1.0348	1.0449	1.0310	1.0503
T_{66}(p.u.)	0.9872	1.0146	1.0449	1.0062
T_{71}(p.u.)	1.0446	0.9632	0.9783	0.9674
T_{73}(p.u.)	0.9250	1.0706	1.0768	1.0587
T_{76}(p.u.)	1.1000	0.9892	1.0272	0.9663
T_{80}(p.u.)	1.1000	1.0041	0.9976	1.0036
Q_{C18}(p.u.)	0.0538	0.1644	0.2193	0.1130
Q_{C25}(p.u.)	0.1161	0.1733	0.2193	0.1375
Q_{C53}(p.u.)	0.1971	0.1435	0.1565	0.1566
G_{pl}(MW)	11.1328	**10.9830**	14.7281	**9.6184**
G_{fc} ($/h)	42150.7986	**41988.2811**	**41672.8007**	45072.2203

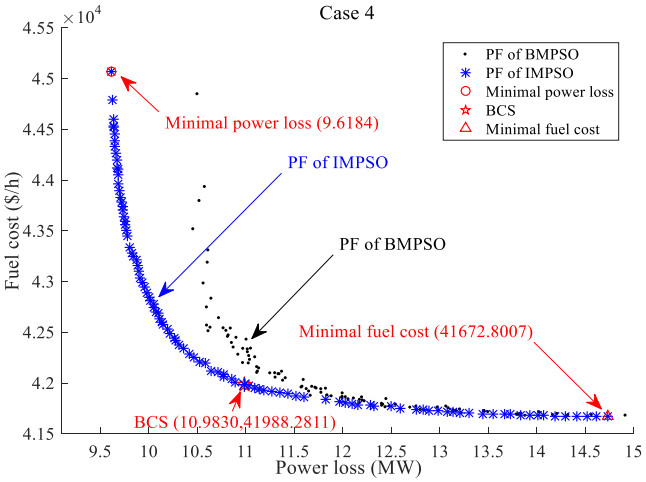

Fig. 6. PF of Case 4

D. Evaluation of IMPSO algorithm

Besides the comparison algorithm BMPSO in this paper, the scheduling schemes of MOOPF problems obtained by proposed IMPSO algorithm are also compared with the recently published results. The comprehensive evaluation based on the single-objective optimal scheduling schemes, the BCS schemes and the operational stability can effectively prove the competitive advantages of IMPSO algorithm.

1) Single-objective optimal scheme

When solving MOOPF problems, IMPSO algorithm can obtain a feasible POS set which is composed of *Np* schemes. TABLE VI gives four minimum single-objective schemes on IEEE 30-bus system obtained by IMPSO algorithm and multiple published results. In detail, the suggested IMPSO algorithm achieves the minimum emission with 0.1942 ton/h, minimum power loss with 2.8410 MW, minimum fuel cost with 799.1717 $/h and minimum fuel cost considering valve-point with 831.3622 $/h. On IEEE 30-bus system, the optimal schemes that only consider single goal obtained by proposed IMPSO algorithm are better than many published methods such as FAHSPSO-DE [6] and INSGA-III [21].

Similarly, TABLE VII gives the comparisons of minimum single-objective schemes on IEEE 57-bus system. It clearly shows that IMPSO algorithm achieves the minimum power loss with 9.6184 MW and minimum fuel cost with 41672.8007 $/h, which dominates multiple published algorithms such as ESDE-MC [9] and DA-PSO [22].

2) BCS scheme

In addition, the BCS scheme is also an intuitive and important indicator to evaluate the performance of different algorithms for solving MOOPF problems.

In this paper, TABLE VIII gives the comparisons of obtained BCS schemes of Case 1 and Case 2 while TABLE IX gives the ones of Case 3 and Case 4. It indicates that the IMPSO algorithm finds the more desirable BCS schemes than most published algorithms such as MPIO-COSR [20] and MFA [5] algorithms. There is no doubt that the comparison results of BCS schemes provide strong persuasion for the superiorities of IMPSO algorithm.

However, there is still room for further improvement in the BCS quality of IMPSO algorithm. For example, TABLE VIII shows that for Case 2, the BCS of IMPSO algorithm is better than the ones of MFA [5] and NHBA-CPFD [18] algorithms. Regrettably, based on the power loss and fuel cost with valve-point, IMPSO algorithm in this paper and NMBAS [11] algorithm do not dominate each other. It is also one of key reasons that BP power flow prediction model is proposed to further optimize BCS and determine WES scheduling schemes.

3) Operational stability

Furthermore, the operational stability of BMPSO and IMPSO algorithms is evaluated based on the PF superposition of 30 independent experiments.

TABLE VI
COMPARISONS OF MINIMUM SINGLE-OBJECTIVE SCHEMES ON IEEE 30-BUS SYSTEM

Algorithm	Emission	Algorithm	Power loss	Algorithms	Fuel cost	Algorithm	Cost with
IMPSO	**0.1942**	**IMPSO**	**2.8410**	**IMPSO**	**799.1717**	**IMPSO**	**831.3622**
INSGA-III[21]	0.1943	INSGA-III[21]	3.1242	INSGA-III[21]	799.5961	IMFO[23]	832.1023
MOIBA[15]	0.20	ESDE-MC[9]	2.8482	HHODE[24]	800.9959	ECHT-DE[16]	832.1356
NISSO[19]	0.2048	MSCA[25]	2.9334	NISSO[19]	799.7624	SF-DE[16]	832.0882
MOEA/D-SF[26]	0.2056	Hybrid DE-HS[27]	3.0542	AMTPG-Jaya[1]	800.1946	SP-DE[16]	832.4813
FAHSPSO-DE[6]	0.2042	AMTPG-Jaya[1]	3.0802	FAHSPSO-DE[6]	799.8066	ACDE[28]	832.0722
ACDE[28]	0.2048	ACDE[28]	3.0840	ACDE[28]	800.4113		
QRJFS[29]	0.204688	QRJFS[29]	2.856711				

TABLE VII
COMPARISONS OF MINIMUM SINGLE-OBJECTIVE SCHEMES ON IEEE 57-BUS SYSTEM

Algorithm	Power loss	Algorithm	Fuel cost
IMPSO	**9.6184**	**IMPSO**	**41672.8007**
ESDE-MC[9]	9.9799	ESDE-EC[9]	41677.7543
DA-PSO[22]	10.1212	DA-PSO[22]	41674.62
FAHSPSO-DE[6]	11.7328	IMOBA[30]	41673
HPSO-DE[6]	11.9788	MOEA/D-SF[26]	41683.39
SMA[31]	10.6734	ISSA[3]	41675.0203
		SMA[31]	41697.1189

TABLE VIII
COMPARISONS OF BCS SCHEMES OF CASE 1 AND CASE 2

Comparisons	Case 1		Comparisons	Case 2	
	Power loss	Fuel cost		Power loss	Fuel cost with valve-point
BMPSO	5.1425	836.4278	BMPSO	5.8706	866.4884
IMPSO	**5.0715**	**831.2837**	**IMPSO**	**5.6685**	**863.3560**
MPIO-COSR[20]	5.1085	831.5576	MFA[5]	5.9195	867.60
HFBA-COFS[32]	5.0796	832.3203	NHBA-CPFD[18]	5.6726	865.9106
INSGA-III[21]	5.0766	832.0140	HFBA-COFS[32]	5.6791	863.7107
MOBBA-CPNS[33]	5.0223	834.6417	NMBAS[11]	5.6487	863.5610

TABLE IX
COMPARISONS OF BCS SCHEMES OF CASE 3 AND CASE 4

Comparisons	Case 3			Comparisons	Case 4	
	Emission	Power loss	Fuel cost		Power loss	Fuel cost
BMPSO	0.2131	4.3964	869.7383	BMPSO	11.1328	42150.7986
IMPSO	**0.2131**	**4.3958**	**863.2721**	**IMPSO**	**10.9830**	**41988.2811**
NSGA-FA[5]	0.2121	4.5558	863.79	ESDE-EC[9]	11.9668	42013.3395
NSGA-III[34]	0.2219	4.8522	873.7811	ESDE-MC[9]	11.8415	41998.3588
I-NSGA-III[34]	0.2218	4.6004	871.0226	HFBA-COFS[32]	10.6995	42122.0140
MPIO-PFM[20]	0.2160	4.4474	866.0601	MOJFS[29]	15.1461	42591.8712

Fig. 7 gives the PF-superposition of BMPSO and IMPSO algorithms for the dual-objective MOOPF case on 30-bus system (Case 1). Fig. 7 intuitively shows that there is almost no difference between 30 PFs obtained by IMPSO algorithm while the 30 PFs of BMPSO algorithm have poor consistency. Meanwhile, Fig. 8 gives the PF-superposition of two involved algorithms for the tri-objective experiment on 30-bus system (Case 3) and Fig. 9 gives the PF-superposition result of a dual-objective MOOPF case on 57-bus system (Case 4).

Fig. 7 ~ Fig. 9 strongly prove that the presented IMPSO algorithm has more significant advantages over the basic BMPSO algorithm in terms of operation stability even on more complex 57-bus system.

IV. BP Prediction Network and Application

Four MOOPF experiments verify that the BCS of proposed IMPSO algorithm is not only superior to the BCS of BMPSO algorithm, but also dominates the ones of most published algorithms. However, further research shows that there is room for further optimization of the BCS quality. Therefore, a multi-output BP prediction model which is suitable for MOOPF problems is proposed in this paper.

A. Proposed BP prediction network

In order to reduce the randomness of experimental results, five candidate BP prediction models are generated according to the main process shown in TABLE X. Then, a relatively optimal BP power flow prediction network is determined from candidate networks based on the mean absolute error (*MAE*), root mean squared error (*RMSE*) and mean absolute percentage error (*MAPE*). Three mentioned errors are shown in (17) ~ (19) [21, 35].

$$MAE = \frac{1}{Np}\sum_{i=1}^{Np}\left|G_{real}(i) - G_{BP}(i)\right| \tag{17}$$

$$RMSE = \sqrt{\frac{\sum_{i=1}^{Np}\left(G_{real}(i) - G_{BP}(i)\right)^2}{Np}} \tag{18}$$

$$MAPE = \frac{1}{Np}\sum_{i=1}^{Np}\left|\frac{G_{real}(i) - G_{BP}(i)}{G_{real}(i)}\right| \times 100\% \tag{19}$$

where G_{real} and G_{BP} are true and predicted goal values.

B. Application of BP network

In this paper, the feasibility of proposed BP power flow prediction model is demonstrated by a dual-objective MOOPF simulation experiment and a tri-objective one.

1) BP network for dual-objective MOOPF

First, a dual output BP prediction model is constructed for Case 1 which optimizes the fuel cost and power loss on IEEE 30-bus system. TABLE XI gives the *RMSE*, *MAE* and *MAPE* errors corresponding to the fuel cost and power loss prediction of five candidate networks. It indicates that the fifth candidate network achieves the smallest prediction errors of G_{fc} and G_{pl} goals, which is adopted as the final BP power flow prediction model of Case 1.

In detail, Fig. 10 gives the fitting results of two goals studied in Case 1 and it clearly shows that the presented BP network can accurately predict fuel cost and power loss based on control variables. The four WES scheduling schemes of Case 1 obtained by BP prediction network are given in TABLE XII. It should be noted that TABLE XII only gives the continuous control variables of WES schemes, while the discrete control variables are the same as the BCS of IMPSO algorithm shown in TABLE II. The fuel cost and power loss goals of WES schemes are both smaller than the ones of BCS determined by IMPSO algorithm, which strongly proves the superiority of BP prediction network.

2) BP network for tri-objective MOOPF

Then, an effective BP power flow prediction network is built for the tri-objective MOOPF Case 3 which optimizes fuel cost, power loss and emission simultaneously.

TABLE XIII gives the evaluation results of five candidate BP networks and the second BP network which realizes the smallest prediction errors is adopted as the final BP power flow prediction model of Case 3. Besides, Fig. 11 gives the fitting results of the predicted fuel cost, power loss, emission and the real ones. Fig. 11 indicates that the BP network built for tri-objective MOOPF problem is not as accurate as the one built for dual-objective MOOPF problem, which points out the direction for further research.

Thrillingly, the proposed BP power flow prediction network is also suitable for the more complex tri-objective MOOPF problem, and successfully obtains three high quality WES schemes shown in TABLE XIV. The WES schemes determined by BP power flow prediction network, which have higher adoption priority than the BCS of IMPSO algorithm, provide multiple satisfactory scheduling schemes for the optimal operation of power system.

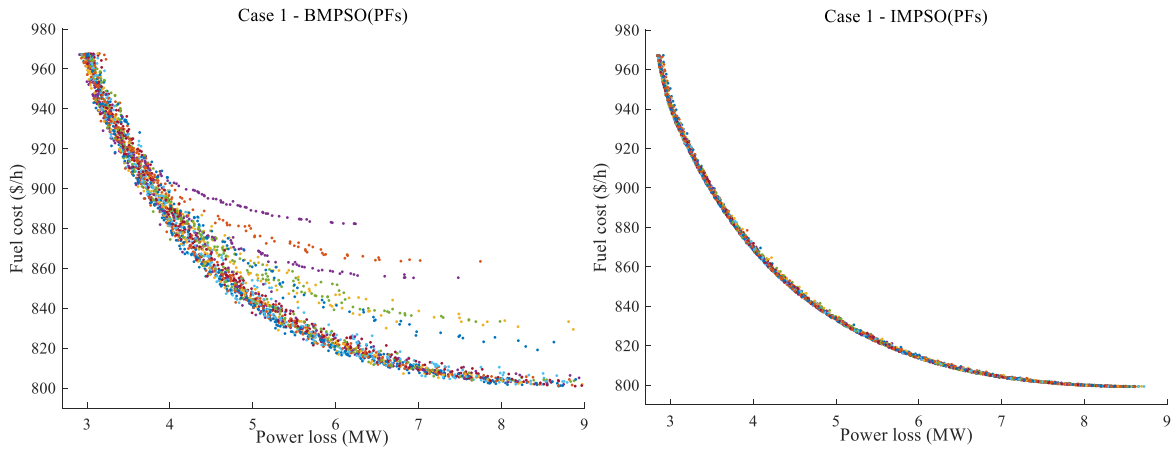

Fig. 7. Superposition of 30 PFs of dual-objective MOOPF on 30-bus system

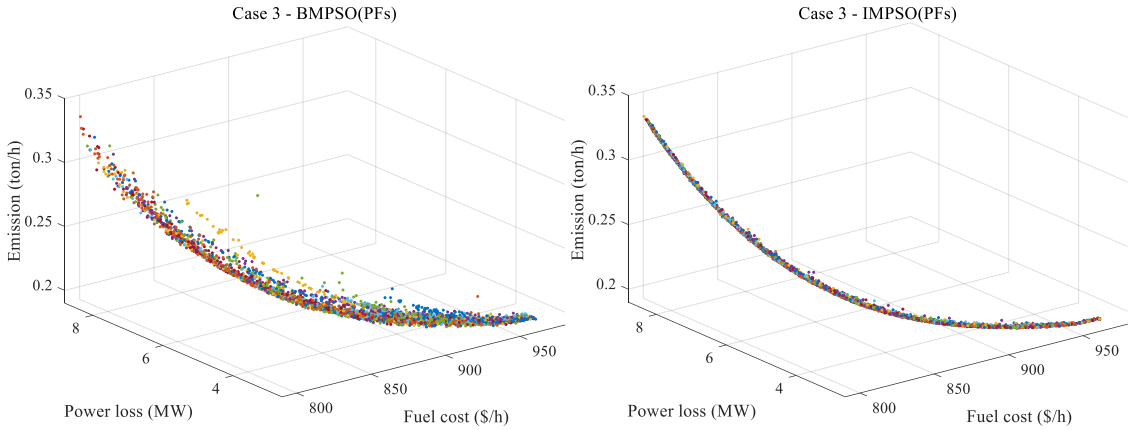

Fig. 8. Superposition of 30 PFs of triple-objective MOOPF on 30-bus system

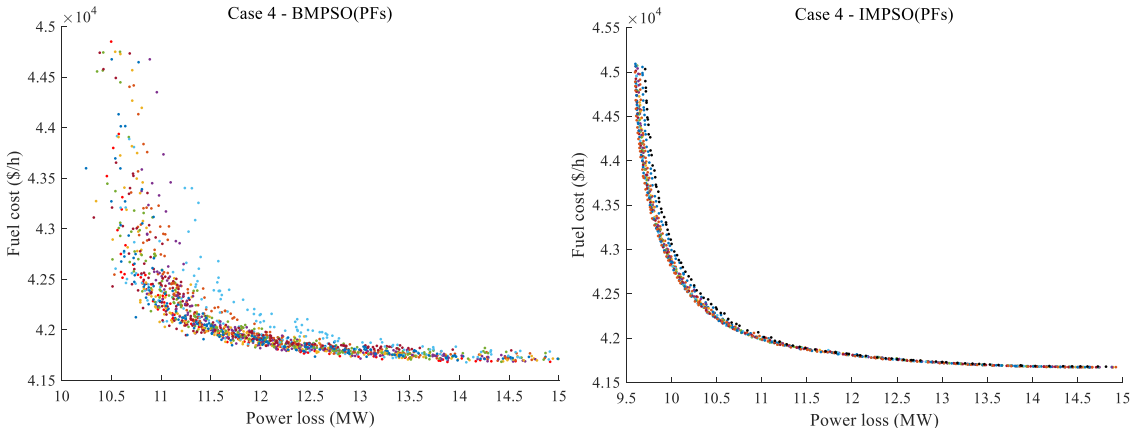

Fig. 9. Superposition of 30 PFs of dual-objective MOOPF on 57-bus system

TABLE X
BP POWER FLOW PREDICTION NETWORK FOR MOOPF PROBLEMS

Begin

Input 1000 scheduling schemes and the corresponding G_e, G_{fc}, G_{fv}, G_{pl} goals

for i=1:5

Select the random 900 schemes for BP network training (In_{train}) and the other 100 schemes for testing (In_{test});

Identify the corresponding output data of training data (Out_{train}) and testingdata (Out_{test});

Perform the data normalization;

Clarify the structure of BP power flow prediction network;

Generate the ith candidate BP prediction network $N_{BP(i)}$;

Predict the m goals of In_{test} set ($OutBP_{test}$) according to $N_{BP(i)}$ model;

Perform the inverse-normalization on $OutBP_{test}$ set to obtain the predictive goals (Pre_{test});

Save the ith BP model $N_{BP(i)}$;

end for

Evaluate the quality of five candidate BP prediction networks based on Out_{test} and Pre_{test};

Determine the relatively-best model N_{BP}^{best} based on *RMSE*, *MAE* and *MAPE* errors;

Input the control variables of BCS scheme determined by IMPSO algorithm (BCS_{IMPSO});

Set the valid ranges of BP exploration operation within [0.999 BCS_{IMPSO}, 1.001 BCS_{IMPSO}];

Randomly generate N_{bp} candidate scheduling schemes within the above valid ranges;

Regulate the mentioned N_{bp} schemes based on (5);

Obtain the predictive G_e, G_{fc}, G_{fv} and G_{pl} goals of N_{bp} schemes based on N_{BP}^{best} network;

Pick out the elite schemes with m smaller goals than the current BCS scheme;

Perform the Newton-Raphson power flow calculation to the above elite schemes and obtain the real G_e, G_{fc}, G_{fv}, G_{pl} goals;

Determine the WES schemes which realize zero constraint-violation and dominate the BCS of IMPSO algorithm;

End

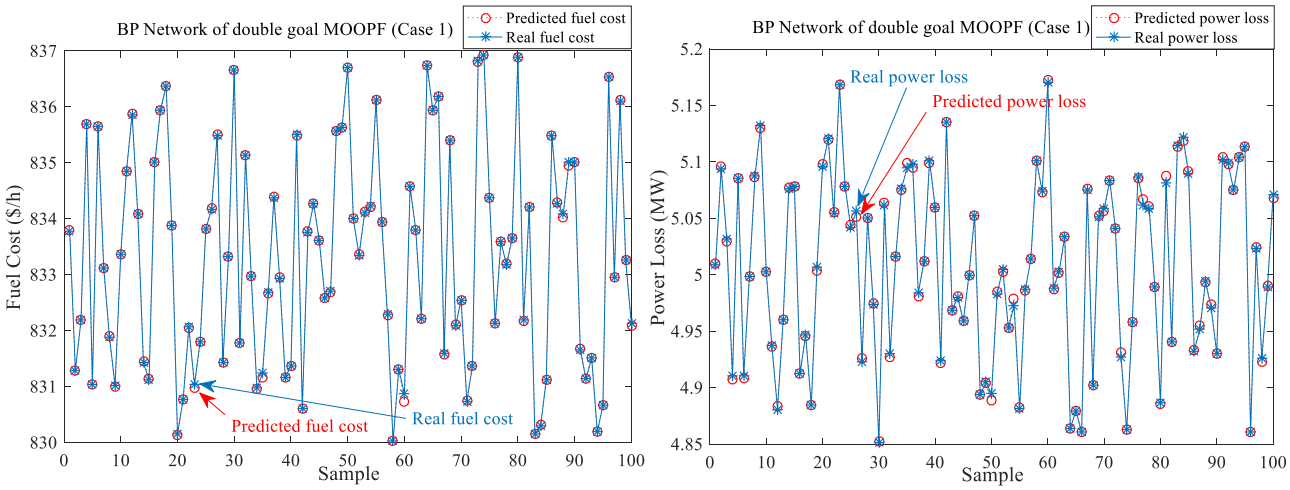

Fig. 10. Fitting results of predicted and real goals of dual-objective Case 1

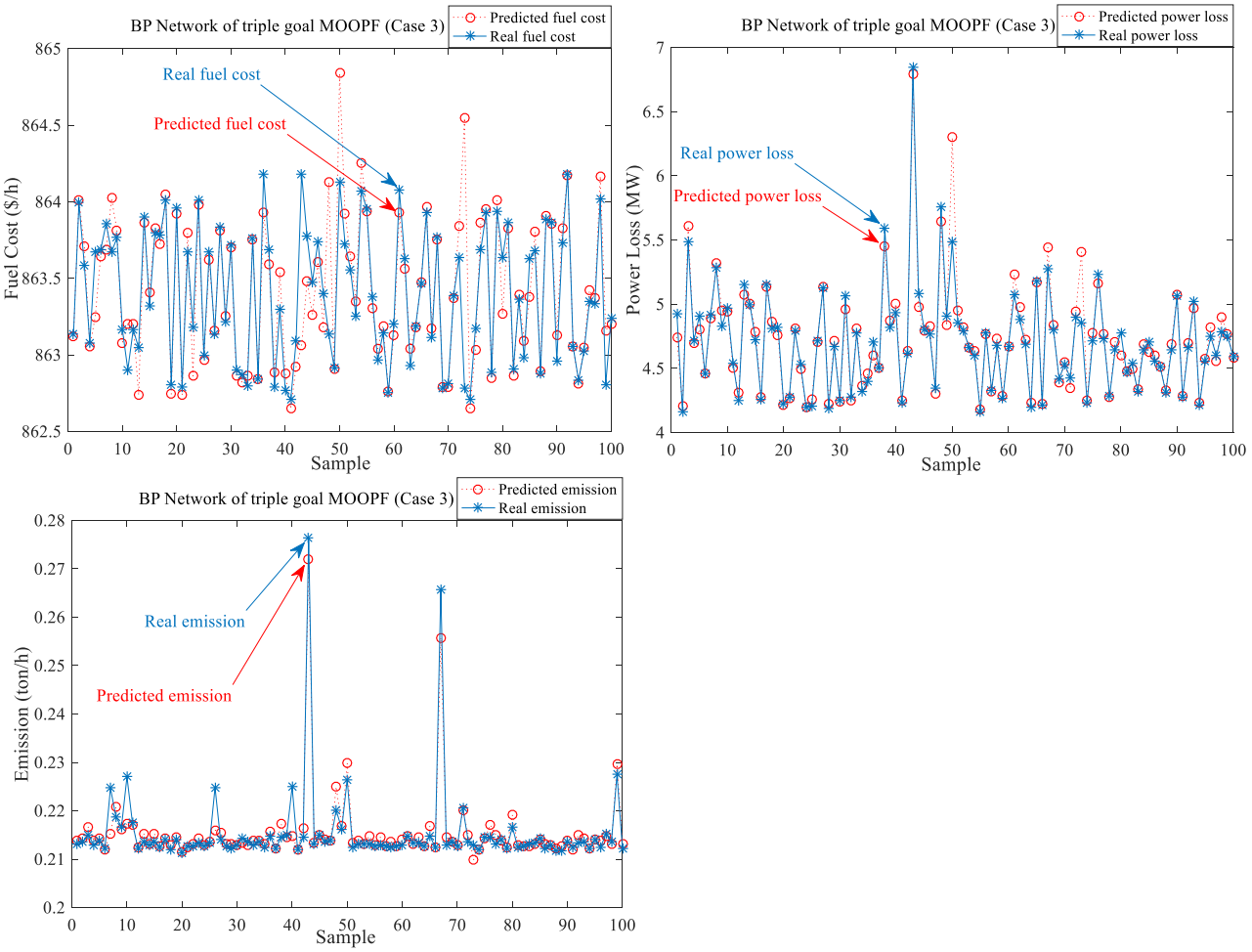

Fig. 11. Fitting results of predicted and real goals of tri-objective Case 3

TABLE XI
PREDICTION ERRORS OF BP NETWORK FOR DUAL-OBJECTIVE MOOPF PROBLEM

Errors	Case 1 - Fuel cost			Case 1 - Power loss		
	RMSE	*MAE*	*MAPE*	*RMSE*	*MAE*	*MAPE*
Network 1	0.0565	0.0229	2.7482E-05	0.0057	0.0022	4.3849E-04
Network 2	0.0683	0.0305	3.6652E-05	0.0030	0.0019	3.7848E-04
Network 3	0.0663	0.0440	5.2813E-05	0.0058	0.0042	8.3856E-04
Network 4	0.2300	0.0641	7.6857E-05	0.0112	0.0038	7.5259E-04
Network 5	**0.0220**	**0.0118**	**1.4133E-05**	**0.0020**	**0.0014**	**2.7511E-04**

TABLE XII
WES SCHEMES OF DUAL-OBJECTIVE CASE 1

WES schemes	WES_1	WES_2	WES_3	WES_4
P_{G2}(MW)	52.8254	52.7750	52.7681	52.7945
P_{G5}(MW)	30.8117	30.8151	30.8217	30.8340
P_{G8}(MW)	34.8115	34.8603	34.8128	34.8312
P_{G11}(MW)	27.6847	27.6881	27.7070	27.6711
P_{G13}(MW)	23.0703	23.0556	23.0601	23.0510
V_{G1}(p.u.)	1.1000	1.1000	1.1000	1.0998
V_{G2}(p.u.)	1.0911	1.0909	1.0910	1.0912
V_{G5}(p.u.)	1.0692	1.0707	1.0693	1.0696
V_{G8}(p.u.)	1.0783	1.0779	1.0778	1.0784
V_{G11}(p.u.)	1.0958	1.0953	1.0954	1.0956
V_{G13}(p.u.)	1.1000	1.1000	1.0991	1.1000
G_{pl}(MW)	**5.0700**	**5.0710**	**5.0714**	**5.0714**
G_{fc} ($/h)	**831.2763**	**831.2825**	**831.2808**	**831.2759**

TABLE XIII
PREDICTION ERRORS OF BP NETWORK FOR TRI-OBJECTIVE MOOPF PROBLEM

Errors	Case 3 - Emission			Case 3 - Power loss			Case 3 - Fuel cost		
	RMSE	*MAE*	*MAPE*	*RMSE*	*MAE*	*MAPE*	*RMSE*	*MAE*	*MAPE*
Network 1	0.0038	0.0025	0.0115	0.2327	0.1637	0.0341	0.4541	0.3833	4.44E-04
Network 2	**0.0025**	**0.0013**	0.0057	**0.1158**	**0.0591**	**0.0121**	**0.3804**	**0.1564**	**1.81E-04**
Network 3	0.0089	0.0020	**0.0038**	0.1358	0.1020	0.0213	0.4062	0.2945	3.41E-04
Network 4	0.0025	0.0014	0.0062	0.1345	0.0855	0.0172	0.3860	0.2230	2.58E-04
Network 5	0.0034	0.0020	0.0092	0.1979	0.1551	0.0322	0.4618	0.3727	4.32E-04

TABLE XIV
WES SCHEMES OF TRI-OBJECTIVE CASE 3

WES schemes	WES_1	WES_2	WES_3
P_{G2}(MW)	62.1317	62.1276	62.1295
P_{G5}(MW)	35.9534	35.9499	35.9523
P_{G8}(MW)	34.4145	34.4141	34.4162
P_{G11}(MW)	29.4704	29.4697	29.4676
P_{G13}(MW)	29.8893	29.8930	29.8898
V_{G1}(p.u.)	1.1000	1.1000	1.0999
V_{G2}(p.u.)	1.0903	1.0902	1.0903
V_{G5}(p.u.)	1.0851	1.0851	1.0852
V_{G8}(p.u.)	1.0861	1.0861	1.0861
V_{G11}(p.u.)	1.0787	1.0787	1.0786
V_{G13}(p.u.)	1.1000	1.1000	1.1000
G_e(ton/h)	**0.2131**	**0.2131**	**0.2131**
G_{pl}(MW)	**4.3943**	**4.3949**	**4.3952**
G_{fc}($/h)	**863.2644**	**863.2562**	**863.2589**

V. CONCLUSION

To explore high-quality dispatching schemes and realize the optimal operation of power system, the innovative IMPSO algorithm and BP power flow prediction network are proposed in this paper.

By integrating constraint-goal dominant strategy, local exploration and mutation-crossover operations, the presented IMPSO algorithm can solve the high dimensional MOOPF problems smoothly. Four MOOPF experiments on different systems verify that IMPSO achieves better PF and BCS than basic BMPSO and published algorithms. Furthermore, the effective BP power flow prediction network suitable for both dual-objective and tri-objective MOOPF problems is put

forward in this paper. Based on the BCS found by IMPSO algorithm, the presented BP prediction network successfully obtains more than three WES scheduling schemes with zero constraint-violation and better performance.

In general, the preferable power flow scheduling schemes determined by proposed IMPSO algorithm and BP prediction network can reduce fuel cost, power loss and emission, which is very valuable for the optimal operation of power system.

REFERENCES

[1] W. Warid, "Optimal power flow using the AMTPG-Jaya algorithm," *Applied Soft Computing*, vol. 91, pp. 106252, 2020.

[2] J. S. Ferreira, E. J. de Oliveira, A. N. de Paula, L. W. de Oliveira, and J. A. Passos Filho, "Optimal power flow with security operation region," *International Journal of Electrical Power & Energy Systems*, vol. 124, pp. 106272, 2021.

[3] S. Abd El-sattar, S. Kamel, M. Ebeed, and F. Jurado, "An improved version of salp swarm algorithm for solving optimal power flow problem," *Soft Computing*, vol. 25, no. 5, pp. 4027-4052, 2021.

[4] W. W, H. Hashim, M. Norman, W. Noor, and I. Abdul, "A novel quasi-oppositional modified Jaya algorithm for multi-objective optimal power flow solution," *Applied Soft Computing*, vol. 65, pp. 360-373, 2018.

[5] G. Guo, J. Qian and S. Li, "Novel many-objective NSGA-FA algorithm to minimize fuel cost, power loss and emission of electric systems," *IAENG International Journal of Computer Science*, vol. 47, no. 4, pp. 634-644, 2020.

[6] E. Naderi, M. Pourakbari-Kasmaei, F. V. Cerna, and M. Lehtonen, "A novel hybrid self-adaptive heuristic algorithm to handle single- and multi-objective optimal power flow problems," *International Journal of Electrical Power & Energy Systems*, vol. 125, pp. 106492, 2021.

[7] X. Kang and D. Pi, "Forecasting satellite power system parameter interval based on relevance vector machine with modified particle swarm optimization," *IAENG International Journal of Computer Science*, vol. 44, no. 1, pp. 68-78, 2017.

[8] Y. Wu and Q. Song, "Improved particle swarm optimization algorithm in power system network reconfiguration," *Mathematical Problems in Engineering*, vol. 2021, no. 9, pp. 5574501, 2021.

[9] H. Pulluri, R. Naresh and V. Sharma, "An enhanced self-adaptive differential evolution based solution methodology for multiobjective optimal power flow," *Applied Soft Computing*, vol. 54, pp. 229-245, 2017.

[10] G. Chen, X. Zhao, K. Peng, P. Zhou, X. Zeng, H. Long, and M. Zou, "Optimized configuration of location and size for DGs and SCs in radial distributed networks based on improved butterfly algorithm," *IAENG International Journal of Applied Mathematics*, vol. 52, no. 1, pp. 81-100, 2022.

[11] J. Qian, P. Wang, C. Pu, and G. Chen, "Joint application of multi-object beetle antennae search algorithm and BAS-BP fuel cost forecast network on optimal active power dispatch problems," *Knowledge Based Systems*, vol. 226, pp. 107149, 2021.

[12] G. Chen, X. Yi, Z. Zhang, and H. Wang, "Applications of multi-objective dimension-based firefly algorithm to optimize the power losses, emission, and cost in power systems," *Applied Soft Computing*, vol. 68, pp. 322-342, 2018.

[13] K. Deb, A. Pratap, S. Agarwal, and T. Meyarivan, "A fast and elitist multiobjective genetic algorithm: NSGA-II," *IEEE Transactions on Evolutionary Computation*, vol. 2, no. 6, pp. 182-197, 2002.

[14] P. C. Roy, K. Deb and M. M. Islam, "An efficient nondominated sorting algorithm for large number of fronts," *IEEE Transactions on Cybernetics*, vol. 49, no. 3, pp. 859-869, 2019.

[15] G. Chen, J. Qian, Z. Zhang, and Z. Sun, "Multi-objective improved bat algorithm for optimizing fuel cost, emission and active power loss in power system," *IAENG International Journal of Computer Science*, vol. 46, no. 1, pp. 118-133, 2019.

[16] P. P. Biswas, P. N. Suganthan, R. Mallipeddi, and G. A. J. Amaratunga, "Optimal power flow solutions using differential evolution algorithm integrated with effective constraint handling techniques," *Engineering Applications of Artificial Intelligence*, vol. 68, pp. 81-100, 2018.

[17] S. Li, W. Gong, L. Wang, X. Yan, and C. Hu, "Optimal power flow by means of improved adaptive differential evolution," *Energy*, vol. 198, pp. 117314, 2020.

[18] G. Chen, J. Qian, Z. Zhang, and Z. Sun, "Applications of novel hybrid bat algorithm with constrained Pareto fuzzy dominant rule on multi objective optimal power flow problems," *IEEE Access*, vol. 7, pp. 52060-52084, 2019.

[19] T. T. Nguyen, "A high performance social spider optimization algorithm for optimal power flow solution with single objective optimization," *Energy*, vol. 171, pp. 218-240, 2019.

[20] G. Chen, J. Qian, Z. Zhang, and S. Li, "Application of modified pigeon-inspired optimization algorithm and constraint-objective sorting rule on multi-objective optimal power flow problem," *Applied Soft Computing*, vol. 92, pp. 106321, 2020.

[21] J. Qian, H. Long, Y. Long, and C. Zhao, "Improved NSGA-III algorithm and BP fuel-cost prediction network for many-objective optimal power flow problems," *IAENG International Journal of Applied Mathematics*, vol. 51, no. 2, pp. 307-320, 2021.

[22] S. Khunkitti, A. Siritaratiwat, S. Premrudeepreechacharn, R. Chatthaworn, and N. Watson, "A hybrid DA-PSO optimization algorithm for multiobjective optimal power flow problems," *Energies*, vol. 11, no. 9, pp. 2270, 2018.

[23] M. A. Taher, S. Kamel, F. Jurado, and M. Ebeed, "An improved moth-flame optimization algorithm for solving optimal power flow problem," *International Transactions on Electrical Energy Systems*, vol. 29, no. 3, pp. e2743, 2018.

[24] S. Birogul, "Hybrid harris hawk optimization based on differential evolution (HHODE) algorithm for optimal power flow problem," *IEEE Access*, vol. 7, pp. 184468-184488, 2019.

[25] A. F. Attia, R. A. El Sehiemy and H. M. Hasanien, "Optimal power flow solution in power systems using a novel Sine-Cosine algorithm," *International Journal of Electrical Power & Energy Systems*, vol. 99, pp. 331-343, 2018.

[26] P. P. Biswas, P. N. Suganthan, R. Mallipeddi, and G. A. J. Amaratunga, "Multi-objective optimal power flow solutions using a constraint handling technique of evolutionary algorithms," *Soft Computing*, vol. 24, no. 4, pp. 2999-3023, 2020.

[27] S. S. Reddy, "Optimal power flow using hybrid differential evolution and harmony search algorithm," *International Journal of Machine Learning and Cybernetics*, vol. 10, no. 5, pp. 1077–1091, 2019.

[28] S. Li, W. Gong, C. Hu, X. Yan, L. Wang, and Q. Gu, "Adaptive constraint differential evolution for optimal power flow," *Energy*, vol. 235, pp. 121362, 2021.

[29] A. M. Shaheen, R. A. El-Sehiemy, M. M. Alharthi, S. S. M. Ghoneim, and A. R. Ginidi, "Multi-objective jellyfish search optimizer for efficient power system operation based on multi-dimensional OPF framework," *Energy*, vol. 237, pp. 121478, 2021.

[30] Y. Yuan, X. Wu, P. Wang, and X. Yuan, "Application of improved bat algorithm in optimal power flow problem," *Applied Intelligence*, vol. 48, no. 8, pp. 2304-2314, 2018.

[31] S. Khunkitti, A. Siritaratiwat and S. Premrudeepreechacharn, "Multi-objective optimal power flow problems based on slime mould algorithm," *Sustainability*, vol. 13, no. 13, pp. 7448, 2021.

[32] G. Chen, J. Qian, Z. Zhang, and Z. Sun, "Multi-objective optimal power flow based on hybrid firefly-bat algorithm and constraints-prior object fuzzy sorting strategy," *IEEE Access*, vol. 7, pp. 139726-139745, 2019.

[33] G. Chen, J. Qian, Z. Zhang, and Z. Sun, "Many-objective new bat algorithm and constraint-priority non-inferior sorting strategy for optimal power flow," *Engineering Letters*, vol. 27, no. 4, pp. 882-892, 2019.

[34] J. Zhang, S. Wang, Q. Tang, Y. Zhou, and T. Zeng, "An improved NSGA-III integrating adaptive elimination strategy to solution of many-objective optimal power flow problems," *Energy*, vol. 172, pp. 945-957, 2019.

[35] C. Liu and M. Jiang, "Robust adaptive filter with lncosh cost," *Signal Processing*, vol. 168, pp. 107348, 2019.